Insulin-modulated Akt subcellular localization determines Akt isoform-specific signaling

Eva Gonzalez and Timothy E. McGraw[1]

Department of Biochemistry, Weill Cornell Medical College, 1300 York Avenue, New York, NY 10065

The 3 Akt protein kinase isoforms have critical and distinct functions in the regulation of metabolism, cell growth, and apoptosis, yet the mechanisms by which their signaling specificity is achieved remain largely unclear. Here, we investigated potential mechanisms underlying Akt isoform functional specificity by using Akt2-specific regulation of glucose transport in insulin-stimulated adipocytes as a model system. We found that insulin activates both Akt1 and Akt2 in adipocytes, but differentially regulates the subcellular distribution of these Akt isoforms. The greater accumulation of Akt2 at the plasma membrane (PM) of insulin-stimulated adipocytes correlates with Akt2-specific regulation of the trafficking of the GLUT4 glucose transporter. Consistent with this pattern, Akt constructs that do not accumulate at the PM to the same degree as Akt2 fail to regulate GLUT4 translocation to the PM, whereas enhancement of Akt1 PM association through mutation in Akt1 PH domain is sufficient to overcome Akt-isoform specificity in GLUT4 regulation. Indeed, we found that this distinct insulin-induced PM accumulation of Akt kinases is translated into a differential regulation by the Akt isoforms of AS160, a RabGAP that regulates GLUT4 trafficking. Our data show that Akt2 specifically regulates AS160 phosphorylation and membrane association providing molecular basis for Akt2 specificity in the modulation of GLUT4 trafficking. Together, our findings reveal the stimulus-induced subcellular compartmentalization of Akt kinases as a mechanism contributing to specify Akt isoform functions.

GLUT4 | AS160 | Akt2 | TBC1D4 | signaling compartmentalization

In response to extracellular stimuli, Akt kinases orchestrate fundamental cellular processes such as metabolism, proliferation and survival (1). Despite a growing knowledge regarding the basic mechanisms of Akt activation (2), how Akt signaling combines versatility and specificity to regulate such a diverse array of cellular functions is largely unknown. Analyses of Akt isoform-specific knockout mice have revealed different physiological roles of the Akt isoforms (3). One of the crucial functions of Akt is the modulation of glucose homeostasis in response to insulin (4), a process that specifically relies on Akt2 (5, 6). Insulin regulates glucose uptake in muscle and fat by inducing the redistribution of the GLUT4 glucose transporter from intracellular sites to the PM (7). Despite the fact that adipocytes express both Akt1 and Akt2, insulin-stimulated GLUT4 translocation and glucose uptake is primarily impaired after Akt2 knockout or knockdown (5, 8–11) [supporting information (SI) Fig. S1 *A and B*]. Moreover, overexpression of Akt2, but not Akt1, rescued impaired insulin-regulated glucose transport in Akt2-null adipocytes (8). However, not all insulin-mediated Akt signaling is isoform specific. For example, both Akt1 and Akt2 have roles in insulin regulation of GSK3β in adipocytes (9) (Fig. S1C). Thus, insulin regulates both Akt1 and Akt2 in adipocytes, leading to common and isoform-specific responses. Akt isoform-specific signaling could arise from various mechanisms, including differences in kinase activation, subcellular localization in response to stimulus, substrate specificity or a combination of those factors. To date the mechanisms that specify Akt isoform specificity in insulin signaling are unknown.

In this study we investigated the mechanisms defining Akt isoform-specific signaling by using Akt2 regulation of insulin-induced glucose transport in adipocytes as a model system. By using quantitative fluorescence microscopy in live adipocytes we found that insulin induces a differential subcellular localization of the Akt1 and Akt2 isoforms. The preferential accumulation of Akt2 at the plasma membrane of insulin-stimulated adipocytes translates into differential substrate specificity and the ability of Akt2 to regulate the trafficking of GLUT4. Therefore, we propose the control of Akt2 subcellular compartmentalization as a mechanism contributing to Akt isoform-specific signaling in adipocytes.

Results and Discussion

Insulin Differentially Regulates the Subcellular Distribution of Akt Isoforms. To investigate the mechanisms underlying Akt isoform specific signaling we measured the activation of Akt1 and Akt2 in response to insulin in 3T3-L1 adipocytes stably expressing Flag epitope-tagged Akt1 or Akt2 (Fig. 1*A*). Akt is activated downstream of PI3-kinase by phosphorylation at Thr$^{308/9}$ and Ser$^{473/4}$ (Akt1 and Akt2, respectively). Both isoforms showed a robust and sustained phosphorylation at these sites (Fig. 1 *B* and *C*). In vitro Akt activity measurements by using a GSK3β fusion peptide revealed that both isoforms were maximally activated after 5 min of insulin stimulation (Fig. 1*D*). Although the activity levels of both isoforms were sustained >30 min, Akt1 activity levels were significantly higher. Consequently, the specific requirement for Akt2 in insulin-induced glucose uptake cannot be explained by a preferential activation of Akt2 by insulin or by the kinetics of Akt2 activation in response to insulin.

It is well known that activation of Akt is mediated by its recruitment and phosphorylation at the PM in response to PI3-kinase activation (12–15). Upon activation, Akt might translocate to different cellular compartments to phosphorylate its substrates (15). We next investigated whether Akt isoform-specific signaling to GLUT4 arises from distinct spatial distributions of the isoforms. We analyzed the effect of insulin on the recruitment and accumulation of Akt1 and Akt2 at the PM of intact adipocytes by using quantitative total internal reflection fluorescence (TIRF) microscopy. In TIRF microscopy only fluorophores within the evanescent field ($\approx$200 nm of the dorsal membrane) are excited, whereas in epifluorescence all fluorophores within cells are excited. The ratio of the TIR fluorescence to epifluorescence per cell is proportional to the fraction of fluorophores located within $\approx$200 nm of the dorsal membrane, thereby providing a quantitative measurement of fluorophores located at the PM environment. In unstimulated (basal) adipocytes, similar fractions of Flag-Akt1 and Flag-Akt2 were in the
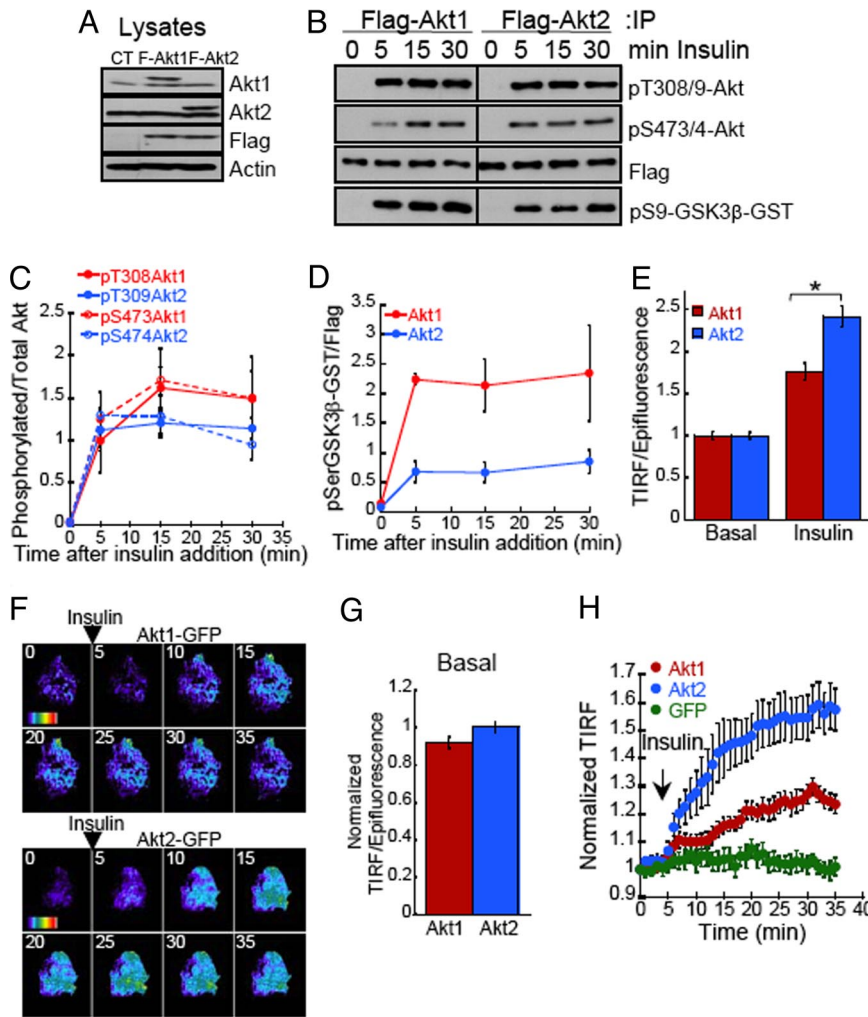

Fig. 1. Insulin differentially regulates the plasma membrane accumulation of Akt isoforms in adipocytes. (*A*) Immunoblot analyses of cell extracts from adipocytes stably expressing Flag-Akt1 or Flag-Akt2. (*B*) Immunoblot analyses of the phosphorylation pattern and in vitro activity of immunoprecipitated Flag-Akt1 or Flag-Akt2 after 10 nM insulin stimulation. In vitro activity kinase assay was performed using as substrate a GST-GSK3β fusion peptide. (*C*) Densitometric analyses of insulin-induced Flag-Akt1 and Flag-Akt2 phosphorylation at Thr$^{308/9}$ and Ser$^{473/4}$. Each data point represents the mean $\pm$ SE, $n = 3$–4. (*D*) Densitometric analyses of in vitro Akt activity measurements. Each data point represents the mean $\pm$ SE, $n = 3$–4. (*E*) Quantification of insulin-induced Flag-Akt1 and Flag-Akt2 redistribution to the PM using TIRF microscopy. Indirect immunofluorescence of the Flag epitope in basal or insulin-stimulated cells was measured in the epifluorescence mode and in the TIRF mode. The TIRF is normalized to the anti-Flag fluorescence in the epifluorescence mode. For each experiment the data are normalized to the basal state of Flag-Akt1 expressing cells. Each data point represents the mean $\pm$ SE, $n \geq 80$ cells. *, $P < 0.001$ (*t* test). (*F*) Time-lapse TIRF microscopy of Akt1-GFP and Akt2-GFP. Images were acquired every min for 35 min, 10 nM insulin was added after 4 min of recording. The average GFP intensity for each cell in the first frame has been subtracted and the pseudo colored images have been equally scaled to allow direct comparison of insulin-induced changes in TIRF for the different constructs. Pseudo color is from purple (low signal) to red (highest signal). (*G*) Quantification Akt1-GFP and Akt2-GFP TIRF versus epifluorescence in live adipocytes in basal conditions. The data are normalized to the Akt2-GFP TIRF/Epifluorescence ratio. Each data point represents the mean $\pm$ SE, $n \geq 120$ cells. (*H*) Quantification of time-lapse TIRF microscopy of GFP, Akt1-GFP, and Akt2-GFP. TIR GFP fluorescence for each cell was measured in every frame, background fluorescence was subtracted and fluorescence was normalized to the first frame TIRF value. The data shown are the mean $\pm$ SE, $n \geq 12$ cells.

evanescence field; however, after insulin stimulation, a significantly greater fraction of Akt2 accumulated at the PM (Fig. 1*E*). The effect of insulin in Akt2 accumulation in the evanescence field was blocked by the PI3-kinase inhibitor wortmannin (Fig. S2), indicating that the changes in Akt accumulation at the PM are in response to PI3-kinase activation.

We next used TIRF microscopy to monitor the accumulation of GFP-tagged Akt isoforms at the PM of live cells (Fig. 1*F*). Serum-starved adipocytes displayed similar fractions of total Akt1-GFP and Akt2-GFP in the vicinity of the PM (Fig. 1*G*); in agreement with our observations in fixed cells using the Flag-tagged Akt constructs (Fig. 1*E*). Insulin-stimulation promoted the redistribution of both isoforms to the PM (Fig. 1*H*, Movie S1 and Movie S2). Importantly, quantification of TIRF

intensity from time-lapse measurements demonstrated that upon stimulation with insulin, Akt2 accumulated at the PM to approximately twice the level of Akt1 (Fig. 1*H*). These results demonstrate a differential effect of insulin on the subcellular localizations of the Akt isoforms.

Akt translocation to the plasma membrane is mediated by PH domain binding to PM phosphadidylinositides (PtdIP3) generated upon PI3-kinase activation (12–14). The PH domain is connected to the catalytic-carboxyl hydrophobic domains of Akt by a linker region (Fig. 2*A*). To determine whether the PH domains are responsible for the differences in Akt isoform PM targeting, we generated constructs containing the PH-linker domains of Akt1 (PHL-Akt1) and Akt2 (PHL-Akt2) (Fig. S3). In unstimulated adipocytes, the PH-linker domain of Akt2 accu-
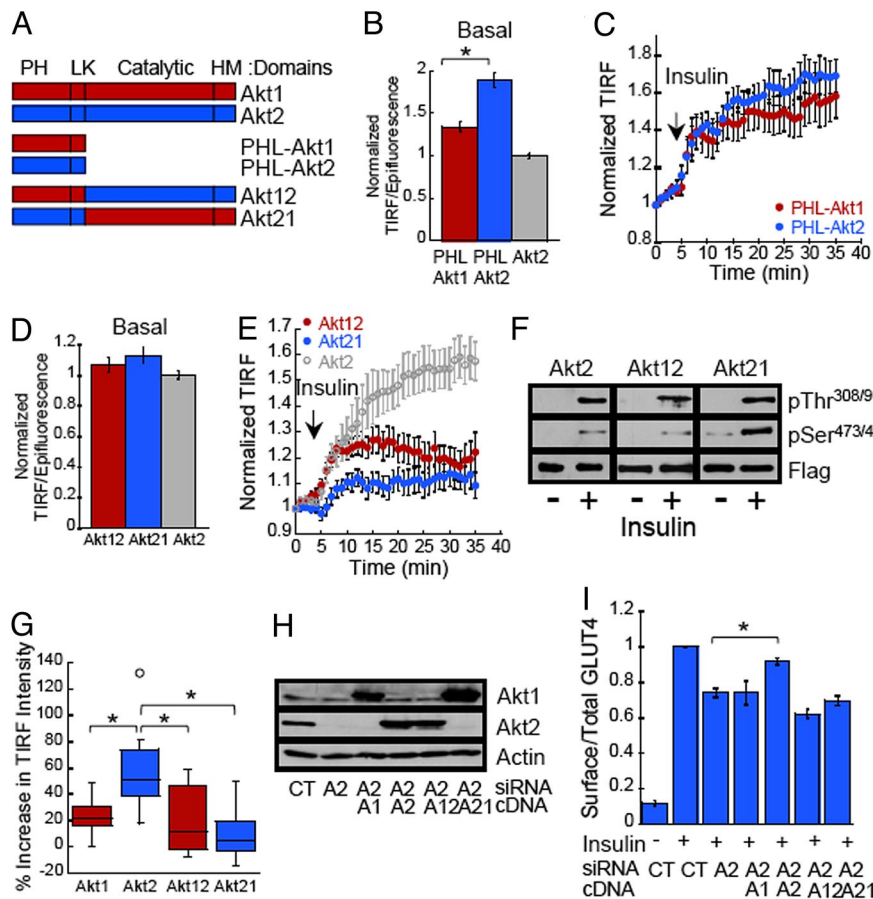
Fig. 2. Insulin-induced accumulation of Akt2 at the PM depends on both the PH-linker and catalytic-regulatory domains and necessary for GLUT4 translocation. (*A*) Schematic representation of Akt constructs tagged with eGFP at the carboxy-terminus. Akt1: full length Akt1; Akt2: full length Akt2; PHL-Akt1: Akt1 residues 1–149; PHL-Akt2 residues 1–151 Akt2; Akt12: chimera Akt1 (1–149)-Akt2 (152–481); Akt21: chimera Akt2 (1–151)-Akt1 (150–480). (*B*) Quantification PHL-Akt1-GFP and PHL-Akt2-GFP TIRF versus epifluorescence in live adipocytes in basal conditions. The data are normalized to the Akt2-GFP TIRF/Epifluorescence ratio. Each data point represents the mean ± SE, $n \geq 76$ cells. *, $P < 0.01$ *t* test. (*C*) Quantification of time-lapse TIRF microscopy of PHL-Akt1-GFP and PHL-Akt2-GFP. Data are process as in Fig. 1*H*. The data shown are the mean ± SE from $n \geq 13$ cells per condition. (*D*) Quantification of Akt12-GFP and Akt21-GFP TIRF versus epifluorescence in living adipocytes in basal conditions. The data are normalized to Akt2-GFP TIRF/Epifluorescence ratio. Each data point represents mean ± SE, $n \geq 77$ cells. (*E*) Quantification of time-lapse TIRF microscopy of Akt12-GFP and Akt21-GFP. Data quantified as described in Fig. 1*H*. Quantification of time-lapse TIRF of Akt2-GFP from Fig. 1*H* has been included for direct comparison. The data shown are the mean ± SE, $n = 12$ cells. (*F*) Immunoblot analyses prepared from 3T3-L1 adipocytes stably expressing Flag-Akt2, Flag-Akt12 or Flag-Akt21. Adipocytes were treated with 10 nM insulin and Akt constructs were immunoprecipitated with an anti-Flag epitope antibody. (*G*) Box-and-whisker diagram showing the increase in TIR fluorescence of GFP tagged Akt constructs in adipocytes after 30 min of insulin stimulation. Data are derived from graphs in Figs. 1*H* and 2*E*. *, $P < 0.001$ (ANOVA). (*H*) Immunoblot analyses of cell extracts prepared from adipocytes coelectroporated with Akt siRNAs and cDNAs as noted. (*I*) Surface-to-total distribution of HA-GLUT4-GFP in adipocytes electroporated with control or Akt2 siRNA and cDNA encoding Akt constructs: A1, Akt1; A2, Akt2; A12, Akt12 chimera; A21, Akt21 chimera. Each bar represents the mean ± SE, $n = 2$–6. In each experiment the surface-to-total GLUT4 distribution was normalized to that of control cells stimulated with 1 nM insulin.

mulated at the PM to a higher extent than that of Akt1 (Fig. 2*B*). Those differences were abolished by wortmannin treatment, indicating that basal PI3-kinase activity is required for the difference in Akt PH-linker domain PM binding in unstimulated cells (Fig. S4). Despite the increased accumulation of PHL-Akt2 at the PM of unstimulated cells, both PHL-Akt1 and PHL-Akt2 constructs were recruited to the PM with indistinguishable kinetics in response to insulin (Fig. 2*C*). It is of interest to note that both the Akt1 and Akt2 PH-linker constructs accumulated to a greater degree at the PM of serum-starved cells than did either full length Akt isoform (Fig. 2*B*). These data indicate that the catalytic-carboxyl hydrophobic domains have a role in reducing Akt PM association in unstimulated cells. The negative contribution of the catalytic-carboxyl hydrophobic domains to Akt PH domain PM targeting might facilitate the inhibition of full length Akt in the absence of stimulus. These observations are consistent with the proposal that inactive Akt is in a "closed" conformation in which the PH and catalytic domains interact.

This conformation would reduce PH domain-mediated PtInsP3 binding at the PM and thereby impede Akt activation (15, 16).

A priori the increased PM targeting of the Akt2 PH-linker domain (Fig. 2*B*) could be responsible for the greater accumulation of Akt2 at the PM of insulin-stimulated cells. To test this hypothesis we characterized the behavior of Akt chimeras in which the PH-linker domains of Akt1 and Akt2 were swapped (Akt12 and Akt21) (Fig. 2*A* and Fig. S3). In serum-starved adipocytes both chimeras accumulated near the PM to the same degree as WT Akt2 (Fig. 2*D*). Both chimeras were recruited to the PM and phosphorylated in response to insulin (Fig. 2 *E* and *F*). However, neither chimera accumulated at the PM in response to insulin to the extent of WT Akt2 (Fig. 2 *E* and *G*). The failure of the Akt21 chimera to recapitulate the insulin-induced PM localization of Akt2 strongly indicates that the Akt2 PH-linker domain by itself does not determine the increased accumulation of Akt2 at the PM of insulin-stimulated adipocytes.

All together our data suggest that in addition to PH domain-

mediated PtInsP3 binding, interactions of other portions of Akt2 with regulatory/effector molecules is crucial in determining the distinct Akt2 PM accumulation. Consistent with our findings, recent studies indicate that structural changes after Akt activation (17) and interactions with regulatory molecules (18, 19) determine Akt subcellular localization. Of particular relevance is the recent report that showed an interaction between Akt catalytic-regulatory domain and ClipR-59 stabilized Akt at the PM upon insulin stimulation (20). Thus, an interaction between Akt2 with ClipR-59 might contribute to the distinct localization of Akt2 at the PM that we demonstrate here.

Our data establish that a single Akt domain does not mediate the preferential accumulation of Akt2 at the PM of insulin-stimulated adipocytes. In contrast to our findings, a recent study has shown that the Akt1 linker domain determines Akt1 targeting to the leading edge of migrating fibroblast (21). These differences in requirements for the targeting of Akt1 and Akt2 to the PM of different cells under different stimuli underscore the complexity of Akt signaling regulation, and suggest that cell type and/or stimulus-specific mechanisms determining Akt isoform-signaling specificity might exist to confer the signaling flexibility required to modulate cellular responses as diverse as cell migration, proliferation or glucose homeostasis.

Insulin-Induced Akt2 Accumulation at the PM Determines Akt2 Specific Regulation of GLUT4 Trafficking. We next sought to investigate whether the distinct PM distribution of the Akt isoforms correlates with the ability of these kinases to regulate GLUT4 trafficking. Insulin-induced GLUT4 translocation is specifically dependent on Akt2-mediated signaling. Therefore, if the greater accumulation of Akt2 at the PM is essential for Akt isoform-specific signaling, then neither Akt1 nor the Akt chimeras, despite being activated by insulin, should signal to GLUT4. To test this hypothesis we determined whether the Akt chimeras would rescue impaired insulin-induced GLUT4 PM translocation in Akt2-knockdown adipocytes. Although, Akt1, Akt2 and both chimeras were well expressed in the Akt2-knockdown adipocytes, only ectopically expressed Akt2 rescued the GLUT4 translocation defect in Akt2-knockdown adipocytes (Fig. 2 *H* and *I*). These results establish that the enhanced accumulation of Akt2 at the PM of adipocytes is necessary for insulin-induced GLUT4 translocation. However, these results do not eliminate the possibility that in addition to stimulus-induced increased PM localization other factors are required for Akt2 specific signaling to GLUT4.

A mutation in the PH domain of Akt1 (Akt1^{E17K}), which leads to pathological accumulation of Akt1 at the PM and enhanced Akt activity, has been identified in human cancers (22). The Akt E^{17}K mutation allows us to further test our hypothesis that insulin-stimulated enrichment of Akt2 at the PM is sufficient for signaling to GLUT4, because our hypothesis predicts that enhanced PM localization of Akt1^{E17K} would overcome Akt isoform specificity in regulation of GLUT4 translocation to the PM. In vitro kinase activity of Flag-tagged Akt1^{E17K} and Akt2^{E17K} mutants isolated from unstimulated adipocytes was significantly higher than that of WT Akt2, demonstrating that the E^{17}K mutation induced basal activation of both isoforms (Fig. 3*A*). Insulin stimulation further increased the activity of the mutants, establishing that the Akt^{E17K} mutants are under dynamic regulation by extracellular stimuli (Fig. 3*A*). In serum-starved adipocytes, both Akt1^{E17K}-GFP and Akt2^{E17K}-GFP accumulated at the PM to a significantly greater extent than WT Akt2-GFP, and insulin stimulated a further increase in Akt1^{E17K} and Akt2^{E17K} at the PM (Fig. 3*B*). The behaviors of the mutant's links increased Akt activity with PM accumulation in both basal and stimulated conditions. Transient over-expression of either Akt1^{E17K} or Akt2^{E17K} induced GLUT4 translocation to the PM in serum-starved adipocytes (Fig. 3 *C* and *D*). The distribution pattern of
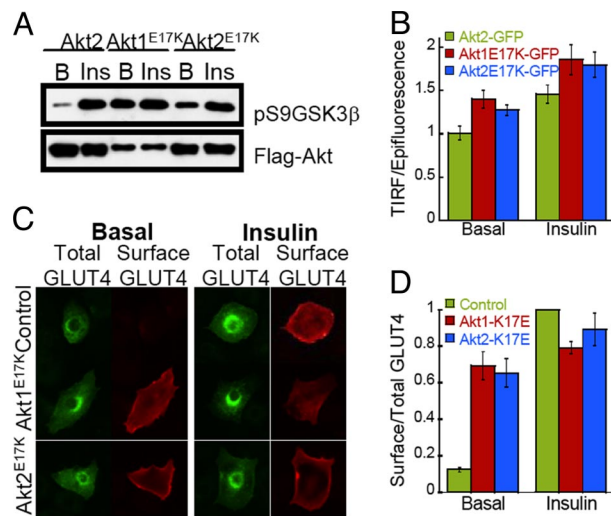

Fig. 3. E17K mutation in Akt1 leads to PM membrane accumulation, activation and GLUT4 translocation. (*A*) The E17K mutation leads to Akt1 and Akt2 activation. Flag-tagged wild type Akt2 and E17K Akt1 and Akt2 mutants were pulled down from unstimulated and 10 nM insulin treated adipocytes and Akt activity was assessed in vitro using GSK3β peptide fused to GST. (*B*) Quantification Akt2-GFP, Akt1^{E17K}-GFP and Akt2^{E17K}-GFP TIRF versus epifluorescence in serum starved and 10 nM insulin treated adipocytes. The data are normalized to the Akt2-GFP basal TIRF/Epifluorescence ratio. Each data point represents the mean $\pm$ SE, $n = 40$ cells. (*C*) Images of HA-GLUT4-GFP cellular distribution in control and Akt E17K mutants expressing adipocytes. (*D*) Surface-to-total distribution of HA-GLUT4-GFP in 3T3-L1 adipocytes electroporated with Akt E17K mutants. Each bar represents the mean $\pm$ SE, $n = 4$. In each experiment data were normalized to that of control cells stimulated with 1 nM insulin.

GLUT4 in unstimulated adipocytes overexpressing Akt1^{E17K} or Akt2^{E17K} mimicked that of insulin-stimulated control cells (Fig. 3*C*). The effect of the E^{17}K mutation documents that enhanced PM targeting of either Akt isoform is sufficient to induce GLUT4 translocation and overcome the Akt2 isoform specificity in the regulation of GLUT4 trafficking. These data combined with the observations that neither WT Akt1 or the Akt chimeras were able to rescue the impairment in GLUT4 translocation in Akt2-knockdown adipocytes, despite being activated by insulin, establish that localized Akt activity at the PM is the critical determinant in Akt2 isoform-specific signaling to GLUT4 trafficking. Past studies have shown that activation of Akt by artificial membrane targeting (that is, PM association that is not determined by Akt PH domain) is sufficient to induce GLUT4 translocation to the PM of adipocytes (23, 24). Our results advance the understanding of Akt regulation and control of GLUT4 translocation by demonstrating that it is the accumulation of activated Akt at the PM and not simply Akt activity that is required for GLUT4 translocation. Furthermore, our data combined with previous studies suggest that the ability of insulin to induce sustained PtdIP3 production (25) and Akt2 PM accumulation (Fig. 1*H*) might represent a critical feature of insulin signaling to regulate GLUT4 trafficking.

Akt2 Specifically Regulates the RabGAP AS160 at the PM Environment. An extension of our hypothesis is that enrichment at the PM should provide Akt2 enhanced access to a substrate(s) required for GLUT4 translocation. Previous studies have shown that Akt-mediated phosphorylation and inhibition of the RabGAP AS160 (also known as TBC1D4) is required for insulin-induced GLUT4 vesicle docking and fusion with the PM (26–28). We next determined the contribution of Akt isoforms in insulin-stimulated phosphorylation of AS160. Consistent with the spe-
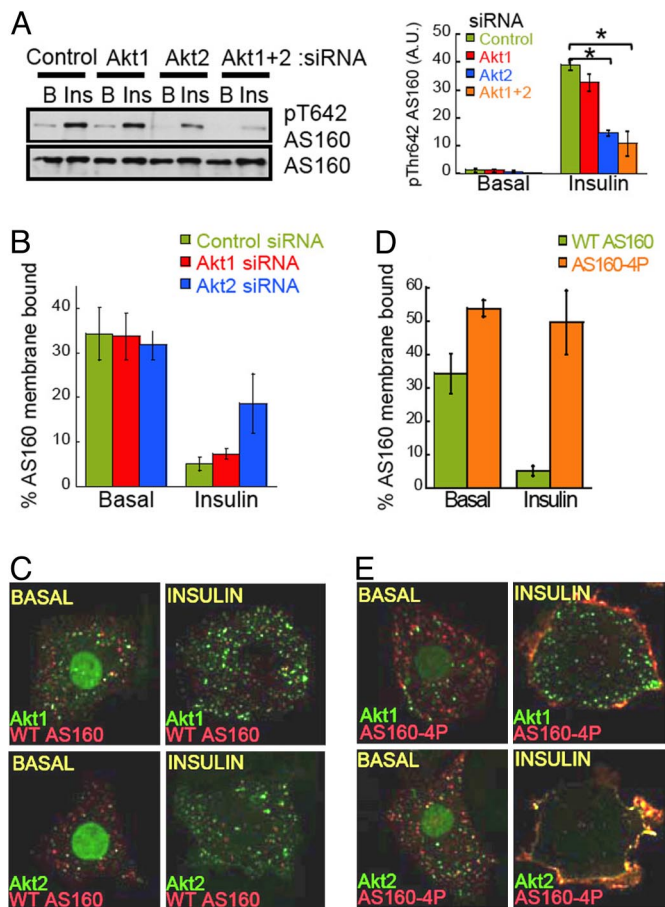
Fig. 4. Akt2 interacts with AS160 at the PM environment and regulates AS160 phosphorylation and membrane release in response to insulin. (*A*) *Left*, immunoblot of AS160 phosphorylation in adipocytes electroporated with noted siRNAs. B, Basal, and Ins, insulin, 10 nM for 15 min. *Right*, densitometric analyses of AS160 phosphorylation. Each data point represents the mean ± SE, $n = 3$. *, $P < 0.05$ (ANOVA). (*B*) Adipocytes electroporated with Flag-AS160, HA-GLUT4-GFP and siRNAs as noted. Serum-starved or insulin stimulated cells were permeabilized for 1 min to leak out cytosolic contents and the amount of membrane bound AS160 was determined by indirect immunofluorescence as described in Methods. (*C*) Confocal images of permeabilized adipocytes overexpressing Akt1-GFP or Akt2-GFP and Flag-AS160 in the absence or presence of 10 nM insulin. The Akt-GFP constructs display some nuclear localization, consistent with previous reports; however, it is of note that this nuclear fraction can be dynamically mobilized upon stimulation. (*D*) Adipocytes were electroporated with Flag-AS160 or Flag-AS160−4P and HA-GLUT4-GFP and membrane bound AS160 was determined as in *B*. Each bar represents the mean ± SE, $n = 3$. (*E*) Confocal images of permeabilized adipocytes overexpressing Akt1-GFP or Akt2-GFP and Flag-AS160−4P in the absence or presence of 10 nM insulin.

cific role of Akt2 in the control of GLUT4 trafficking, knock-down of Akt2 but not Akt1 blunted insulin-stimulated phosphorylation of AS160 (Fig. 4*A*). Biochemical studies have shown that AS160 interacts with cellular membranes, including GLUT4 vesicles and, that insulin-induced AS160 phosphorylation can trigger its membrane dissociation (29). This release of AS160 from membranes might relieve the inhibition of Rab proteins, including Rab10 that control GLUT4 translocation (28, 30). We next characterized the role of Akt isoforms in the regulation of AS160 membrane targeting. To measure membrane associated AS160 we used a quantitative microscopy assay in which cells are detergent permeabilized before fixation to leak out soluble cytosolic contents (31). Consistent with biochemical studies, AS160 association with cellular membranes was reduced

by insulin-stimulation (Fig. 4*B*). Importantly, the effect of insulin on AS160 membrane association was blunted by knockdown of Akt2 but not Akt1 (Fig. 4*B*). Thus, Akt2 specifically regulates the phosphorylation and membrane release of AS160 in response to insulin, providing a molecular explanation for Akt isoform-specific signaling to GLUT4.

To investigate the site of interaction between Akt and AS160 in insulin-stimulated adipocytes, we examined in confocal microscopy the localization of AS160 and Akt isoforms in membrane compartments of permeabilized cells. In unstimulated adipocytes, both Akt1 and Akt2 partially colocalized with AS160 in vesicle structures throughout the cell (Fig. 4*C*). Previous studies have shown that the dynamic association of Akt with discrete endosomal populations might be important for aspects of Akt signal transduction (31, 32). However, we did not observe a significant increase in the colocalizations of Akt and AS160 upon insulin treatment in intracellular vesicles (Fig. 4*C*). Unlike our results using TIRF microscopy in live cells (e.g., Fig. 1*F*), in the permeabilized cell assay no accumulation of either Akt isoform at the PM was observed (Fig. 4*C*). Because of the different lipid compositions of the PM and cytoplasmic membranes, permeabilization with saponin differentially affects the integrity and protein binding to those membranes. Therefore, these results suggest that the accumulation of Akt isoforms at the PM is dynamic and this association with the PM is not preserved in adipocytes permeabilized before fixation, consistent with previous observations in HeLa cells (31). Consequently, both the dynamics of Akt association with the PM and the release of AS160 from membranes upon phosphorylation (Fig. 4*B*) limit our ability to detect Akt and AS160 colocalization at the PM of insulin-stimulated permeabilized cells.

In an attempt to overcome the dynamic interaction of Akt and AS160 with cellular membranes, we used a phosphorylation deficient mutant of AS160 (AS160−4P) to stabilize the interactions of Akt2 and AS160 at cellular membranes. In this AS160 mutant 4 of the Akt phosphorylation sites are changed to alanines and its overexpression is known to inhibit GLUT4 translocation (26). Consistent with our observation in Fig. 4*B* and recent biochemical data supporting that insulin-induced AS160 phosphorylation controls AS160 membrane association (29), insulin did not promote the release of AS160−4P from membranes of permeabilized adipocytes (Fig. 4*D*). In serum-starved permeabilized adipocytes, both Akt1 and Akt2 display limited colocalization with AS160−4P in vesicle structures throughout the cell (11.8 ± 1.7% Akt1 colocalization with AS160, 18.9 ± 3.4% Akt2 colocalization with AS160), in patterns similar to those observed in cells coexpressing WT AS160 (Fig. 4 *C* and *E*). Insulin stimulation induced a dramatic redistribution of AS160−4P to the PM environment. Importantly, in insulin-stimulated adipocytes, Akt2 significantly accumulated at the PM along with AS160−4P, with little Akt2 remaining on other intracellular membranes (Fig. 4*E*, 69.6 ± 2.8% Akt2 colocalization with AS160−4P). The effect of AS160−4P was specific for Akt2 because there was only a minor redistribution of Akt1 to the PM in insulin-stimulated adipocytes coexpressing AS160−4P. A significant fraction of Akt1 remained at intracellular vesicles depleted of AS160−4P (Fig. 4*E*, 29 ± 5% Akt1 colocalization with AS160−4P). The observation that Akt2 and AS160−4P colocalize at the PM environment of insulin-stimulated cells further supports our hypothesis that Akt2 accumulation at the PM facilitates regulation of downstream targets required for GLUT4 translocation. In sum, our findings show that the distinct insulin-induced PM accumulation of Akt2 is translated into a differential regulation of AS160 by the Akt isoforms. The specific regulation of AS160 phosphorylation and membrane association by Akt2 provides a molecular link for Akt2 specificity in the regulation of GLUT4 trafficking.

Our data reveal that extracellular stimuli can induce the

simultaneous activation but differential subcellular localization of Akt family members, leading to distinct regulation of downstream effectors and therefore cellular functions. Given the high signaling potential of Akt kinases, the spatial restriction of Akt isoform signaling might be crucial to integrate in a regulated manner growth, survival, and metabolic responses induced by hormones and growth factors. Conversely, alterations in Akt subcellular localization such as those caused by mutations in Akt PH domain, or upstream regulators of Akt membrane recruitment, like PI3-kinase or PTEN, which are commonly present in human cancers (33), might lead to deregulation of Akt isoform functional specificity and it will be of interest to investigate the contribution of this alteration to the transforming phenotype caused by those mutations.

Methods

Antibodies and *siRNA*. For detailed information see *SI Text*.

Molecular Cloning. Wild type mouse Akt1-YFP and Akt2-YFP were obtained from ATCC and use as templates to generate all Akt constructs described. Cloning procedures are described in *SI Text*. Flag-tagged wild type AS160 and AS160–4P (AS160 mutated to alanine at Ser^{318}, Ser^{588}, Thr^{642}, Ser^{751}) constructs have been described (26)and were a gift from Dr Lienhard (Dartmouth Medical School).

Cell Culture, Adipocyte Differentiation and Retroviral Infection and Electroporation. 3T3-L1 fibroblasts were cultured, differentiated into adipocytes and electroporated as described in ref. 34. For detailed information see *SI Text*.

Immunoblot Analyses and Immunoprecipitation. For full description see *SI Text*. In vitro Akt activity assay- 3T3-L1 adipocytes expressing Flag-tagged Akt constructs were starved in SF-DMEM for 2–4 h. After insulin stimulation, Flag-tagged Akt constructs were immunoprecipitated using anti-Flag M2 antibody. Immunocomplexes were assayed for Akt activity using reagents and following the protocol provided by Cell Signaling Technologies. For detailed information see *SI Text*.

GLUT4 Translocation. The HA-GLUT4-GFP reporter contains an exofacial HA epitope, therefore the increase of HA-GLUT4-GFP at the PM is measured as an increase in HA epitope fluorescence in nonpermeabilized cells. HA-GLUT4-GFP translocation has been described in detail (35). For rescue experiments cells were coelectroporated with Akt2 specific siRNA and plasmids encoding HA-GLUT4-GFP and Flag-tagged Akt constructs. After staining with anti-HA antibody in nonpermeabilizing conditions, cells were incubated with anti-Flag epitope antibody in PBS-5% calf serum-250 μm/mL saponin to assess coexpression of GLUT4 and Akt constructs.

Fluorescence Quantification. MetaMorph software (Universal Imaging, West Chester, PA) was used for image processing and quantification as described in ref. 36. For detailed information see *SI Text*.

Total Internal Reflection Fluorescence (TIRF) Microscopy. To perform ''prismless'' TIRF microscopy a 60 × 1.45 numerical aperture oil-immersion objective (Olympus America, Melville, NY) was used. The evanescent field decay length was 100–250 nm, with a pixel size of 112 × 112 nm^2 in the acquired images. For detailed information TIRF data collection and analysis, see *SI Text*.

Determination of Membrane Bound AS160 in Intact Cells. 3T3-L1 adipocytes were electroporated with plasmids encoding Flag-tagged AS160 (wild type or AS160–4P mutant) and HA-GLUT4-GFP in combination with control, Akt1 or Akt2 specific siRNA. Forty-eight hours after electroporation cells were starved for 2–4 h in serum free DMEM followed by 15 min insulin stimulation. Cells were washed with cold Media 1 and permeabilized with Pipes 80 mM (pH 6.8), EGTA 5 mM, MgCl2 1 mM, saponin 0.05% for 1min to leak out the cytosolic contents (31, 36). Cells were fixed in 3.7% formaldehyde and stained with anti-Flag antibody to detect membrane-bound AS160. To asses total expression of the constructs some dishes were fixed without permeabilization. Samples were imaged in epifluorescence mode. The average fluorescence intensity of Flag-tagged AS160 was normalized to the average fluorescence intensity of GLUT4 for each sample. The membrane bound fraction of AS160 was determined by the ratio between AS160 normalized fluorescence intensity in permeabilized versus nonpermeabilized cells.

Statistics Analysis. Student's paired *t* test and ANOVA test were used for data statistical analysis as noted.

1. Manning BD, Cantley LC (2007) AKT/PKB signaling: Navigating downstream. *Cell* 129:1261–1274.
2. Woodgett JR (2005) Recent advances in the protein kinase B signaling pathway. *Curr Opin Cell Biol* 17:150–157.
3. Dummler B, Hemmings BA (2007) Physiological roles of PKB/Akt isoforms in development and disease. *Biochem Soc Trans* 35(Pt 2):231–235.
4. Whiteman EL, Cho H, Birnbaum MJ (2002) Role of Akt/protein kinase B in metabolism. *Trends Endocrinol Metab* 13:444–451.
5. Cho H, et al. (2001) Insulin resistance and a diabetes mellitus-like syndrome in mice lacking the protein kinase Akt2 (PKB beta). *Science* 292:1728–1731.
6. Garofalo RS, et al. (2003) Severe diabetes, age-dependent loss of adipose tissue, and mild growth deficiency in mice lacking Akt2/PKB beta. *J Clin Invest* 112:197–208.
7. Huang S, Czech MP (2007) The GLUT4 glucose transporter. *Cell Metab* 5:237–252.
8. Bae SS, Cho H, Mu J, Birnbaum MJ (2003) Isoform-specific regulation of insulin-dependent glucose uptake by Akt/protein kinase B. *J Biol Chem* 278:49530–49536.
9. Jiang ZY, et al. (2003) Insulin signaling through Akt/protein kinase B analyzed by small interfering RNA-mediated gene silencing. *Proc Natl Acad Sci USA* 100:7569–7574.
10. Katome T, et al. (2003) Use of RNA interference-mediated gene silencing and adenoviral overexpression to elucidate the roles of AKT/protein kinase B isoforms in insulin actions. *J Biol Chem* 278:28312–28323.
11. Gonzalez E, McGraw TE (2006) Insulin Signaling Diverges into Akt-dependent and -independent Signals to Regulate the Recruitment/Docking and the Fusion of GLUT4 Vesicles to the Plasma Membrane. *Mol Biol Cell* 17:4484–4493.
12. Bellacosa A, et al. (1998) Akt activation by growth factors is a multiple-step process: The role of the PH domain. *Oncogene* 17:313–325.
13. Andjelkovic M, et al. (1997) Role of translocation in the activation and function of protein kinase B. *J Biol Chem* 272:31515–31524.
14. Ananthanarayanan B, Ni Q, Zhang J (2005) Signal propagation from membrane messengers to nuclear effectors revealed by reporters of phosphoinositide dynamics and Akt activity. *Proc Natl Acad Sci USA* 102:15081–15086.
15. Bellacosa A, Kumar CC, Di Cristofano A, Testa JR (2005) Activation of AKT kinases in cancer: Implications for therapeutic targeting. *Adv Cancer Res* 94:29–86.
16. Calleja V, et al. (2007) Intramolecular and intermolecular interactions of protein kinase B define its activation in vivo. *PLoS Biology* 5:e95.
17. Ananthanarayanan B, Fosbrink M, Rahdar M, Zhang J (2007) Live-cell molecular analysis of Akt activation reveals roles for activation loop phosphorylation. *J Biol Chem* 282:36634–36641.
18. Maira SM, et al. (2001) Carboxyl-terminal modulator protein (CTMP), a negative regulator of PKB/Akt and v-Akt at the plasma membrane. *Science* 294:374–380.
19. Higuchi M, Onishi K, Kikuchi C, Gotoh Y (2008) Scaffolding function of PAK in the PDK1-Akt pathway. *Nat Cell Biol* 10:1356–1364.
20. Ding J, Du K (2009) ClipR-59 interacts with Akt and regulates Akt cellular compartmentalization. *Mol Cell Biol* 29:1457–1471.
21. Kim EK, et al. (2008) Linker region of Akt1/protein kinase Balpha mediates platelet-derived growth factor-induced translocation and cell migration. *Cell Signal* 20(11):2030–2037.
22. Carpten JD, et al. (2007) A transforming mutation in the pleckstrin homology domain of AKT1 in cancer. *Nature* 448:439–444.
23. Ng Y, Ramm G, Lopez JA, James DE (2008) Rapid activation of Akt2 is sufficient to stimulate GLUT4 translocation in 3T3–L1 adipocytes. *Cell Metab* 7:348–356.
24. Kohn AD, Summers SA, Birnbaum MJ, Roth RA (1996) Expression of a constitutively active Akt Ser/Thr kinase in 3T3–L1 adipocytes stimulates glucose uptake and glucose transporter 4 translocation. *J Biol Chem* 271:31372–31378.
25. Tengholm A, Meyer T (2002) A PI3-kinase signaling code for insulin-triggered insertion of glucose transporters into the plasma membrane. *Curr Biol* 12:1871–1876.
26. Sano H, et al. (2003) Insulin-stimulated phosphorylation of a Rab GTPase-activating protein regulates GLUT4 translocation. *J Biol Chem* 278:14599–14602.
27. Eguez L, et al. (2005) Full intracellular retention of GLUT4 requires AS160 Rab GTPase activating protein. *Cell Metab* 2:263–272.
28. Larance M, et al. (2005) Characterization of the role of the Rab GTPase-activating protein AS160 in insulin-regulated GLUT4 trafficking. *J Biol Chem* 280:37803–37813.
29. Stockli J, et al. (2008) Regulation of glucose transporter 4 translocation by the Rab guanosine triphosphatase-activating protein AS160/TBC1D4: Role of phosphorylation and membrane association. *Mol Endocrinol* 22:2703–2715.
30. Sano H, et al. (2007) Rab10 is a target of the insulin regulated AS160 rabGAP protein required for insulin-stimulated translocation of GLUT4 to the plasma membrane of adipocytes. *Cell Metab* 5:293–303.
31. Schenck A, et al. (2008) The endosomal protein Appl1 mediates Akt substrate specificity and cell survival in vertebrate development. *Cell* 133:486–497.
32. Saito T, Jones CC, Huang S, Czech MP, Pilch PF (2007) The interaction of Akt with APPL1 is required for insulin-stimulated Glut4 translocation. *J Biol Chem* 282:32280–32287.
33. Carnero A, Blanco-Aparicio C, Renner O, Link W, Leal JF (2008) The PTEN/PI3K/AKT signalling pathway in cancer, therapeutic implications. *Current Cancer Drug Targets* 8:187–198.
34. Zeigerer A, et al. (2002) GLUT4 retention in adipocytes requires two intracellular insulin-regulated transport steps. *Mol Biol Cell* 13:2421–2435.
35. Lampson MA, Schmoranzer J, Zeigerer A, Simon SM, McGraw TE (2001) Insulin-regulated release from the endosomal recycling compartment is regulated by budding of specialized vesicles. *Mol Biol Cell* 12(11):3489–3501.
36. Stenmark H, et al. (1994) Inhibition of rab5 GTPase activity stimulates membrane fusion in endocytosis. *EMBO J* 13:1287–1296.

CELL BIOLOGY